Biomedical Optics EXPRESS

Correlating optical coherence elastography based strain measurements with collagen content of the human ovarian tissue

Sreyankar Nandy,[1] Hassan S. Salehi,[2] Tianheng Wang,[2] Xiaohong Wang,[3] Melinda Sanders,[3] Angela Kueck,[4] Molly Brewer,[4] and Quing Zhu[1,2,*]

[1]*University of Connecticut, Department of Biomedical Engineering, Storrs, CT 06269, USA*
[2]*University of Connecticut, Department of Electrical and Computer Engineering, Storrs, CT 06269, USA*
[3]*University of Connecticut Health Center, Division of Pathology, Farmington, CT 06030, USA*
[4]*University of Connecticut Health Center, Division of Gynecologic Oncology, Farmington, CT 06030, USA*
**zhu@engr.uconn.edu*

Abstract: In this manuscript, the initial feasibility of a catheter based phase stabilized swept source optical coherence tomography (OCT) system was studied for characterization of the strain inside different human ovarian tissue groups. The ovarian tissue samples were periodically compressed with 500 Hz square wave signal along the axial direction between the surface of an unfocused transducer and a glass cover slide. The displacement and corresponding strain were calculated during loading from different locations for each tissue sample. A total of 27 *ex vivo* ovaries from 16 patients were investigated. Statistically significant difference ($p < 0.001$) was observed between the average displacement and strain of the normal and malignant tissue groups. A sensitivity of 93.2% and a specificity of 83% were achieved using 25 microstrain (με) as the threshold. The collagen content of the tissues was quantified from the Sirius Red stained histological sections. The average collagen area fraction (CAF) obtained from the tissue groups were found to have a strong negative correlation ($R = -0.75$, $p < 0.0001$) with the amount of strain inside the tissue. This indicates much softer and degenerated tissue structure for the malignant ovaries as compared to the dense, collagen rich structure of the normal ovarian tissue. The initial results indicate that the swept source OCT system can be useful for estimating the elasticity of the human ovarian tissue.

OCIS codes: (110.4500) Optical coherence tomography; (170.6935) Tissue characterization; (170.3890) Medical optics instrumentation; (170.4440) ObGyn; (170.1610) Clinical applications.

References and links

1. T. R. Rebbeck, H. T. Lynch, S. L. Neuhausen, S. A. Narod, L. Van't Veer, J. E. Garber, G. Evans, C. Isaacs, M. B. Daly, E. Matloff, O. I. Olopade, and B. L. Weber, "Prevention and observation of surgical end points study group prophylactic oophorectomy in carriers of BRCA1 or BRCA2 mutations," N. Engl. J. Med. **346**(21), 1616–1622 (2002).
2. W. A. Rocca, B. R. Grossardt, M. de Andrade, G. D. Malkasian, and L. J. Melton 3rd, "Survival patterns after oophorectomy in premenopausal women: a population-based cohort study," Lancet Oncol. **7**(10), 821–828 (2006).
3. A. K. Lind, B. Weijdegård, P. Dahm-Kähler, J. Mölne, K. Sundfeldt, and M. Brännström, "Collagens in the human ovary and their changes in the perifollicular stroma during ovulation," Acta Obstet. Gynecol. Scand. **85**(12), 1476–1484 (2006).
4. T. Wang, M. Brewer, and Q. Zhu, "An overview of optical coherence tomography for ovarian tissue imaging and characterization," Nanomed. Nanobiotechnol. **7**(1), 1–16 (2015).
5. J. Schmitt, "OCT elastography: imaging microscopic deformation and strain of tissue," Opt. Express **3**(6), 199–211 (1998).

#245807 Received 13 Jul 2015; revised 27 Aug 2015; accepted 30 Aug 2015; published 3 Sep 2015

6. R. K. Wang, Z. H. Ma, and S. J. Kirkpatrick, "Tissue Doppler optical coherence elastography for real time strain rate and strain mapping of soft tissue," Appl. Phys. Lett. **89**(14), 144103 (2006).
7. W. Qi, R. Chen, L. Chou, G. Liu, J. Zhang, Q. Zhou, and Z. Chen, "Phase-resolved acoustic radiation force optical coherence elastography," J. Biomed. Opt. **17**(11), 110505 (2012).
8. J. Zhu, Y. Qu, T. Ma, R. Li, Y. Du, S. Huang, K. K. Shung, Q. Zhou, and Z. Chen, "Imaging and characterizing shear wave and shear modulus under orthogonal acoustic radiation force excitation using OCT Doppler variance method," Opt. Lett. **40**(9), 2099–2102 (2015).
9. R. K. Wang, S. Kirkpatrick, and M. Hinds, "Phase-sensitive optical coherence elastography for mapping tissue microstrains in real time," Appl. Phys. Lett. **90**(16), 164105 (2007).
10. G. Guan, C. Li, Y. Ling, Y. Yang, J. B. Vorstius, R. P. Keatch, R. K. Wang, and Z. Huang, "Quantitative evaluation of degenerated tendon model using combined optical coherence elastography and acoustic radiation force method," J. Biomed. Opt. **18**(11), 111417 (2013).
11. W. Xu, R. Mezencev, B. Kim, L. Wang, J. McDonald, and T. Sulchek, "Cell stiffness Is a Biomarker of the Metastatic Potential of Ovarian Cancer Cells," PLoS One **7**(10), e46609 (2012).
12. G. Liu, O. Tan, S. S. Gao, A. D. Pechauer, B. Lee, C. D. Lu, J. G. Fujimoto, and D. Huang, "Postprocessing algorithms to minimize fixed-pattern artifact and reduce trigger jitter in swept source optical coherence tomography," Opt. Express **23**(8), 9824–9834 (2015).
13. R. K. Manapuram, S. R. Aglyamov, F. M. Monediado, M. Mashiatulla, J. Li, S. Y. Emelianov, and K. V. Larin, "*In vivo* estimation of elastic wave parameters using phase-stabilized swept source optical coherence elastography," J. Biomed. Opt. **17**(10), 100501 (2012).
14. K. M. Kennedy, R. A. McLaughlin, B. F. Kennedy, A. Tien, B. Latham, C. M. Saunders, and D. D. Sampson, "Needle optical coherence elastography for the measurement of microscale mechanical contrast deep within human breast tissues," J. Biomed. Opt. **18**(12), 121510 (2013).
15. M. Razani, A. Mariampillai, C. Sun, T. W. H. Luk, V. X. D. Yang, and M. C. Kolios, "Feasibility of optical coherence elastography measurements of shear wave propagation in homogeneous tissue equivalent phantoms," Biomed. Opt. Express **3**(5), 972–980 (2012).
16. S. J. Kirkpatrick, R. K. Wang, and D. D. Duncan, "OCT-based elastography for large and small deformations," Opt. Express **14**(24), 11585–11597 (2006).
17. W. Malkusch, B. Rehn, and J. Bruch, "Advantages of Sirius Red staining for quantitative morphometric collagen measurements in lungs," Exp. Lung Res. **21**(1), 67–77 (1995).
18. E. Gheorghe, V. Tomuţa, T. Mehedinţi, M. Hîncu, and V. Broască, "Comparative microscopic study of the ovarian blood vessels," Rom. J. Morphol. Embryol. **48**(2), 151–154 (2007).
19. O. Dzatic-Smiljkovic, M. Vasiljevic, M. Djukic, R. Vugdelic, and J. Vugdelic, "Frequency of ovarian endometriosis in epithelial ovarian cancer patients," Clin. Exp. Obstet. Gynecol. **38**(4), 394–398 (2011).

1. Introduction

Ovarian cancer has the highest mortality rate among all the gynecological cancers. This can be mainly attributed to the late stage of detection (mainly stage III and IV) due to lack of effective early screening and diagnostic techniques. Currently, prophylactic oophorectomy (PO) is accepted as the standard procedure for high risk women [1]. Although PO can reduce the risk of ovarian cancer by more than 50%, the mortality rate of women undergoing premenopausal oophorectomy seems to be considerably increased [2]. As a result, there is an urgent need to develop more sensitive tools for effective evaluation of the ovary during minimally invasive surgery and detection of early stage ovarian cancers.

Collagen is the main structural protein component of the extracellular matrix of the ovarian tissue [3]. Previous studies from optical coherence tomography (OCT) have shown that the collagen content can be a useful marker for detection of ovarian cancer [4]. Optical coherence elastography (OCE) is an extension of conventional OCT, which can measure the micro-mechanical properties of biological tissues [5, 6]. The main principal of OCE is to apply a load to the biological tissue, either through acoustic radiation force (ARF) and measure the quantitative elastic modulus [7, 8], or measure displacement and strain, which can then be used to characterize the tissue elasticity [9, 10]. 95% of the ovarian cancer originates from the epithelial layer cells on the outer surface of the ovarian tissue, which makes the malignant ovarian tissue surface much softer compared to the normal tissue [11]. Thus the relative difference in stiffness is expected to provide the mechanical contrast between healthy and malignant ovarian tissues for diagnosis.

We report in this paper, to the best of our knowledge, the first exploratory study showing the feasibility of a catheter based phase stabilized swept source OCT system for estimating the strain inside human ovarian tissue and also measure the correlation between the measured

#245807 Received 13 Jul 2015; revised 27 Aug 2015; accepted 30 Aug 2015; published 3 Sep 2015

strain with the ovarian tissue collagen content. A total of 27 *ex vivo* ovaries obtained from 16 patients were investigated. Ovarian tissue samples were placed between an unfocused transducer and a glass slide. A square wave signal (500 Hz, 50% duty cycle), co-registered with the OCT data acquisition system was used to periodically compress the tissue sample between the transducer surface and the cover slide along the axial direction. The displacement inside the tissue was calculated from the phase difference between the pre-compression and post compression A-line measurements. The average local strain was calculated by least square fitting of the displacement curve.

2. Materials and methods

2.1 Phase stabilized swept source OCE

Figure 1 illustrates the technical details of the phase stabilized swept source OCE system, which is based on a 1310 nm swept source (HSL-2000, Santec Corp., Japan) with a bandwidth of 110 nm and scan rate of 20 kHz. The 10 mW output power from the swept source was evenly split into reference and sample arms by a 2 × 2 coupler. The backscattered light was collected by a side view ball lens catheter (WT&T Inc., Canada, diameter 0.5 mm) and recombined with the reference light at the second 2 × 2 coupler. The interference signal was detected by a balanced detector (Thorlabs PDB120C) and acquired by a 50 MHz digitizer (Cs8325, Gage Applied) after a 20 MHz anti-alias filter. The axial resolution of the system in air was 12μm at a distance of 1mm from the focus. The phase jitter of the swept source was removed by using a narrow band fiber bragg grating (OE Land, λo = 1310 nm, $\Delta\lambda$ = 0.096 nm, reflectivity> 99%) as the trigger for A-scan acquisition. The phase stability of the swept source OCT system was measured to be ~7 mrads, which correspond to a displacement sensitivity of 1.4 nm in air.

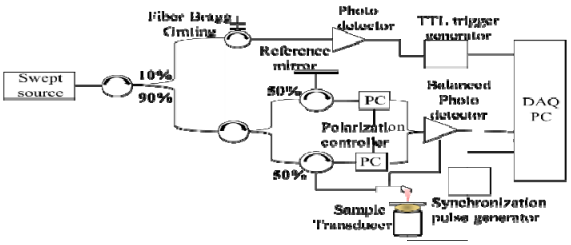

Fig. 1. Swept source optical coherence elastography configuration.

2.2 Calculation of displacement and strain

Ovarian tissue samples were placed between an unfocused transducer (Krautkramer Alpha) and a cover slide of thickness 140 μm. This transducer has a frequency response from several Hz to 300 KHz. A square wave (500 Hz, 50% duty cycle), generated by a function generator synchronized with the data acquisition system was used to periodically compress the sample in the axial direction between the transducer surface and the glass cover slide. For most of the imaging purposes, the catheter probe was kept fixed (no axial scanning) and M-mode images were acquired. 600 A-lines were averaged for each M-mode image to reduce the effect of any residual sample arm jitter and to improve the SNR of the measured displacement. The acquisition time for each M-mode image was 30 ms. The displacement amplitude and corresponding strain was calculated from 50~100 locations, at a separation of 5μm depending on the size of ovary sample. The overall acquisition time for each ovary sample was < 1 sec, which makes the system suitable for potential *in vivo* applications. An example of a normal and malignant ovarian tissue is shown in Fig. 2. The representative B-scan images of the normal and malignant samples are shown in Fig. 2(a) and Fig. 2(e). The white dashed rectangular area in the B-scan images represent the area from which M-mode images were acquired as shown in Fig. 2(b) and Fig. 2(f) respectively. The displacement at each location is

#245807 Received 13 Jul 2015; revised 27 Aug 2015; accepted 30 Aug 2015; published 3 Sep 2015

measured from the phase difference between the pre-compression and post-compression A-lines. The strain inside the tissue can be estimated from the slope of the displacement curve. The average displacement was estimated for each sample and the corresponding average strain was calculated by linear least square fitting of the displacement curve, as shown in Fig. 2(d) and Fig. 2(h). Phase stability of an endoscopic swept source OCE system can be challenging due to the jitter induced by the trigger and slow linear/rotational scanning movement of the stepper motor [12]. Using the M mode detection scheme, a rapid estimation of overall tissue elasticity can be obtained [13, 14]. It should be noted though that the measured strain is dependent on the experimental conditions, and a strict quantification of the elasticity of the ovarian tissue can only be done by exact measurement of the Young's modulus [15]. However, assuming a uniform distribution of stress throughout the sample, the displacement and strain can provide the corresponding relative mechanical contrast, comparable to the elastic moduli [16].

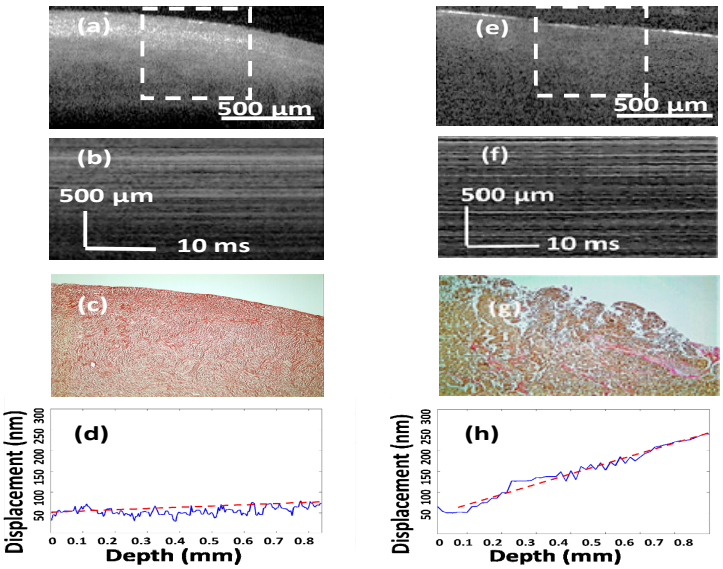

Fig. 2. Examples from normal [(a) - (d)] and malignant [(e) - (h)] ovarian tissue. (a) and (e) OCT B-scan images, the white dashed area representing the locations from which M-mode images were acquired, (b) and (f) M-mode images, (c) and (g) SR stains showing collagen distribution, (d) and (h) corresponding averaged displacement curves. Slopes of the least square fitted red dashed lines in (d) and (h) represent the average strain.

2.3 Human ovary study

Ovary samples were obtained from patients undergoing PO at the University of Connecticut Health Center (UCHC). The patients were at risk for ovarian cancer or they had an ovarian mass suggestive of malignancy. This study was approved by the Institutional Review Boards (IRB) of UCHC, and informed consent was obtained from all patients. A total of 27 ovaries from 16 patients (aged 39–76 years; mean, 57 years) were imaged. The ovarian tissues were diagnosed based on histopathology as normal (n = 22), abnormal (n = 2), and malignant (n = 3). Ovaries were kept in 0.9% wt/vol NaCl solution and imaged fresh within 24 hours after oophorectomy. After OCT imaging, the ovaries were fixed in 10% formalin solution and returned to the Pathology Department for histological processing.

2.4 Histology and collagen area fraction

After the imaging, the ovary samples were cut in 5 mm blocks parallel to the imaging plane, dehydrated with graded alcohol, embedded in paraffin and sectioned to 7 µm thickness using

#245807 Received 13 Jul 2015; revised 27 Aug 2015; accepted 30 Aug 2015; published 3 Sep 2015

a paraffin microtome. The slides that correspond to the imaged planes were identified, and stained using hematoxylin and eosin (H&E) for diagnosis. For quantification of the collagen content inside the tissue, adjacent cross-section (7 μm apart from H&E cross-section) was sliced and stained with Sirius Red, which specifically binds to tissue collagen [17]. The digital image of the surface histology covering about 1mm x1mm area was acquired using a bright field microscope, shown in Fig. 2(c) and Fig. 2(g). The amount of collagen was quantified using ImageJ software. The collagen area fraction (CAF) was measured as "stained collagen area/tissue area."

3. Results and discussions

The H&E histology and Sirius Red stain of the normal ovarian samples exhibited homogeneous and compact collagen distribution. The group of ovaries with abnormal diagnosis consisted of surface endometriosis with trace amount of dense stroma, while the malignant ovarian tissue group consisted of serous carcinoma, severe necrosis and characterized by highly degenerated and scattered collagen distribution. Elastin, another similar protein which might be responsible for tissue elasticity was generally found to be absent in the ovarian stroma [18].

The local strain was measured for a total of 1670 locations, including 1215 from normal, 175 from abnormal and 280 from malignant ovaries. The histograms of the percentage of observations of με are shown in Fig. 3(a), along with Gaussian fitting to show the general trend for each tissue group. The average strain obtained for the normal tissue group was 23.05 με (± 10.74), while the average strain of the abnormal and malignant group was 42.3 με (± 11.11) and 54.14 με (± 11.68), respectively. The ratio of the average strain of the malignant and normal tissue groups was 2.35, signifying much softer tissue structure in the malignant ovaries. The comparison between normal, abnormal and malignant groups by Student's t-test is shown in Fig. 3(b). The difference between the normal-malignant ($p < 0.001$) and normal-abnormal ($p < 0.001$) was found to be highly statistically significant. The comparison between the abnormal and malignant group, though significant, was much closer ($p = 0.047$). This can be attributed to the fact that the abnormal samples consisted of endometriosis, which may have significant association with the development of certain types of ovarian cancers [19] and causes alterations in the connective tissue of the ovary. The receiver operating characteristic (ROC) curve which plots the true positive ratio (TPR) versus false positive ratio (FPR) between the normal and malignant groups is shown in Fig. 3(c). The area under the curve (AUC) is 0.902. Using 25 με as the threshold, a sensitivity of 93.2% and a specificity of 83% was achieved.

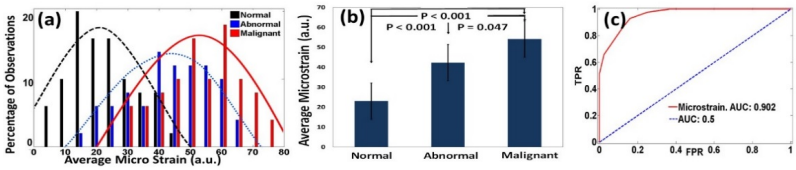

Fig. 3. (a) Histograms of με obtained from normal, abnormal and malignant ovarian tissue groups, along with Gaussian distribution fits. (b) Statistics of normal, abnormal and malignant groups. (c) ROC curve of με.

Figure 4(a) shows the histograms of CAFs obtained from normal, abnormal and malignant ovarian tissue groups. The average CAF of normal group was 47.4% (± 12.3%), while the average CAF of the abnormal and malignant group was 19.85% (± 7.25%) and 10.11% (± 3.22%). The statistical significance between these groups is shown in Fig. 4(b). The ROC curve obtained from the CAF as shown in Fig. 4(c). A sensitivity of 95% and a specificity of 100% were obtained by using 22% CAF as an optimum threshold. The AUC obtained from CAF is 0.988.

#245807 Received 13 Jul 2015; revised 27 Aug 2015; accepted 30 Aug 2015; published 3 Sep 2015

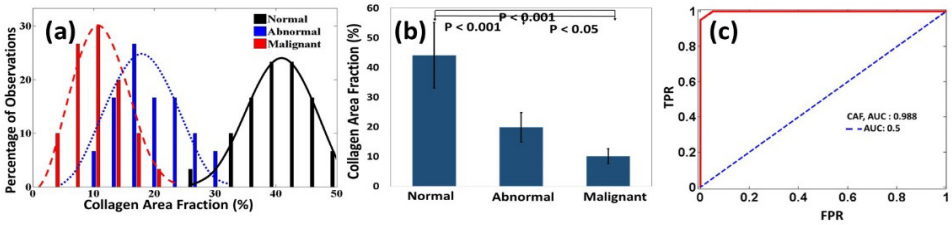

Fig. 4. (a) Histograms of CAF obtained from normal, abnormal and malignant ovarian tissue groups, along with Gaussian distribution fits. (b) Statistics of normal, abnormal and malignant groups. (c) ROC curve of CAF.

A linear regression analysis shown in Fig. 5 demonstrates strong negative correlation ($R = -0.75$, $p < 0.0001$) between the collagen content inside the ovarian tissue and average micro-strain. A highly mature, dense distribution of collagen fibers provides much higher stiffness to the normal ovarian tissue, whereas for endometriosis and development of epithelial ovarian cancer, the collagen structure gradually degenerates and in effect the ovarian tissue becomes much softer and deformable. The current study, though limited by the transmission geometry, shows the initial feasibility of utilizing a catheter based swept source OCT system for elastography measurements of the ovarian tissue. An integrated catheter probe with a ring transducer for loading and imaging from the same side could be potentially useful for *in vivo* applications.

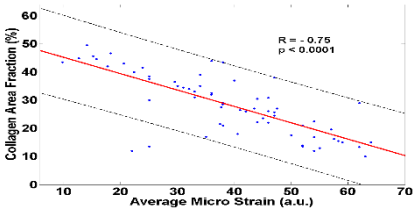

Fig. 5. Negative correlation demonstrated between estimated strain and tissue collagen content. The black dashed lines show 95% prediction intervals.

4. Summary

In this study, 27 ovary samples obtained from 16 patients were studied *ex vivo* using the phase stabilized swept source OCE system. Average displacement amplitude was estimated inside the tissue samples from the phase difference of the pre-compression and post-compression A-lines. The average strain was calculated by linear least square fitting of the displacement curve. A sensitivity of 93.2% and a specificity of 83% were achieved for the normal and malignant tissue groups using strain as a classifier. The collagen content inside the tissue was quantified by Sirius Red staining, and found to have a strong negative correlation with the average strain, indicating a softer and degenerated tissue structure in the malignant group as compared to the normal ovarian tissue. The initial results indicate that the swept source OCE system can be a robust method for ovarian cancer detection and diagnosis and a potential guidance tool for surgeons during minimally invasive surgery.

Acknowledgments

This research was supported by NIH R01CA151570. The authors thank Dr. Yi Yang for helpful discussions on phase stability of the OCE system. The authors also thank Karen Metersky for consenting patients and Melissa Parente for coordinating the tissue sample study.